

Large scale separation and hadronic resonances from a new strongly interacting sector

A. Hasenfratz,¹ C. Rebbi,² and O. Witzel³

¹*Department of Physics, University of Colorado, Boulder, CO 80309, USA*

²*Department of Physics and Center for Computational Science, Boston University, Boston, MA 02215, USA*

³*Higgs Centre for Theoretical Physics, School of Physics & Astronomy, The University of Edinburgh, Edinburgh, EH9 3FD, UK*
(Dated: March 9, 2022)

Many theories describing physics beyond the Standard Model rely on a large separation of scales. Large scale separation arises in models with mass-split flavors if the system is conformal in the ultraviolet but chirally broken in the infrared. Because of the conformal fixed point, these systems exhibit hyperscaling and a highly constrained resonance spectrum. We derive hyperscaling relations and investigate the realization of one such system with four light and eight heavy flavors. Our numerical simulations confirm that both light-light and heavy-heavy resonance masses show hyperscaling and depend only on the ratio of the light and heavy flavor masses. The heavy-heavy spectrum is qualitatively different from QCD and exhibits quarkonia with masses not proportional to the constituent quark mass. These resonances are only a few times heavier than the light-light ones, which would put them within reach of the LHC.

I. INTRODUCTION

Various analysis of data accumulated by ATLAS and CMS in 2016 were recently presented at ICHEP (see e.g. [1, 2]), yet these analysis do not reveal strong evidence for beyond-Standard Model (BSM) phenomena. Nevertheless the Standard Model (SM) is undoubtedly only an effective model. New interactions are necessary to avoid triviality of the scalar sector, describe dark matter or explain neutrino physics, UV complete the Higgs sector, etc. Many viable BSM models rely on large scale separation between the infrared (IR) and ultraviolet (UV) physics [3–9]. Such a scenario naturally leads to a “walking” gauge coupling and provides a dynamical mechanism for electroweak (EW) symmetry breaking, avoiding unnaturally large tuning of the Higgs mass, while satisfying stringent EW precision measurement constraints.

A possibility to achieve large scale separation is to add fermions that are not or only partially gauged under the SM. In this paper we investigate non-perturbative properties of one specific realization. In the UV we start with a gauge system and N_f flavors within the conformal window and drive the system into the chirally broken regime by lifting the mass of some flavors. The energy scale of chiral symmetry breaking is determined by the mass of the heavy flavors. We do not explore the mechanism generating the mass of the heavy flavors but note that by tuning that mass the UV and IR scales can be separated arbitrarily. The UV dynamics is dominated by the conformal infrared fixed point (IRFP) guaranteeing hyperscaling and high predictability of the resonance spectrum made up of both light and heavy flavors. In Reference [7] we investigated such a system with $N_f = 12$ fermions, splitting the masses into $N_\ell = 4$ light and $N_h = 8$ heavy flavors. We showed that if the system in the $m_\ell = m_h = 0$ limit is conformal, it exhibits hyperscaling in m_h in the $m_\ell = 0$ chiral limit. Our numerical results verified this expectation. We also found that the light resonance spectrum of the $4\ell + 8h$ system contained

a relatively light 0^{++} state (i.e. significantly lighter than the vector meson), while the rest of the masses interpolated between the $N_f = 12$ and $N_f = 4$ limits. Further details on the lattice implementation and simulations can be found in [7, 10, 11].

Here we significantly extend our understanding of the $N_f = 4\ell + 8h$ model. In Sect. II we generalize the original derivation of Ref. [7] and deduce that universal hyperscaling should hold in the light-light, heavy-light, and heavy-heavy sector not only in the $m_\ell = 0$ chiral limit but more generally as function of m_ℓ/m_h . These results describe general properties of quantum field theories that are defined in the basin of attraction of a conformal IRFP. In particular, ratios of hadron masses or hadron mass over decay constants as function of m_ℓ/m_h are expected to follow a common functional form, independent of the individual values of the masses. In the basin of attraction of the conformal fixed point, the gauge coupling is irrelevant and the infinite cutoff continuum limit is reached as $m_h \rightarrow 0$. Physical predictions are independent of the gauge coupling when m_h goes to zero.

In Sect. III we verify these expectations in numerical simulations and show that dimensionless ratios depend on m_ℓ/m_h even when varying the gauge coupling. We find that the heavy-heavy resonance states remain relatively light, only a couple of times heavier than the light-light spectrum. This feature is very different from QCD where the heavy-heavy spectrum of the strange, charm, or bottom mesons depend strongly on the quark masses. Depending on how the SM is coupled to the IR system, the resonance states of the $N_f = 4 + 8$ model could be in the few TeV range and therefore accessible at the LHC.

There are many phenomenological models that can be described by systems similar to ours. The first “walking” models emerged in the context of technicolor theories and assumed that the new BSM physics is described by a near-conformal but chirally broken gauge-fermion system. The massless pions couple to the SM fields and break electroweak symmetry, while the Higgs boson might emerge as a regular 0^{++} bound state of the

system [12–18]. It is far from certain that any system is close enough to the conformal window to exhibit the necessary “walking” behavior and large mass anomalous dimension, yet there is indication from lattice studies that near-conformal models can have light 0^{++} states, often referred to as “dilaton-like” Higgs bosons, as they might emerge from a broken scale symmetry [19–25]. Composite Higgs models offer an alternative scenario. In the IR these models are chirally broken with massless Goldstone pions. Coupling to the SM fields breaks the vacuum alignment and lifts some of the pion masses and the Higgs boson emerges as a pseudo Nambu-Goldstone boson (pNGB) [26–34]. Particularly well studied is the minimal scenario based on an $SU(2)$ gauge theory with two Dirac flavors see e.g. [35–37]. Adding heavy flavors will make both the dilaton-like and the pNGB Higgs systems conformal in the UV. The heavy mass controls the “walking” behavior and anomalous dimensions are determined by the IRFP. While the heavy flavors do not effect the light-light spectrum strongly, the heavy-light and heavy-heavy resonances would however be experimentally observable.

Fermion masses in both scenarios are generated either via 4-fermion interactions or partial compositeness. Both mechanisms might require UV properties similar to conformal systems as well. The new composite sector has to be coupled to the SM see e.g. [32]. This leads to a radiative potential for the Higgs as pNGB and thus contributes to the mass of the Goldstone bosons. Other interactions like top-Yukawa couplings could also be significant. In the following we focus on the new strongly interacting sector in isolation and leave investigations of couplings to the SM for future investigations.

II. HYPERSCALING IN MASS-SPLIT SYSTEMS

Hyperscaling in mass-split systems in the basin of attraction of a conformal IRFP follows from Wilsonian renormalization group considerations. For concreteness we assume lattice regularization and work with bare parameters that, inside the conformal window, can be separated into irrelevant gauge couplings g_i and relevant lattice masses $\hat{m}_i = am_i$. The critical surface is given by $\hat{m}_i = 0$ where the system is conformal at the IRFP g_i^* .

In the vicinity of the IRFP an RG transformation that changes the scale $\mu \rightarrow \mu' = \mu/b$ ($b > 1$) drives the gauge couplings to g_i^* , while masses transform with the scaling dimension $y_m = 1 + \gamma_m$ as $\hat{m}_i \rightarrow \hat{m}_i' = b^{y_m} \hat{m}_i$ with γ_m the universal anomalous dimension at the IRFP. The correlation function of an operator H , after rescaling all dimensional quantities by b , change as

$$C_H(t; g_i, \hat{m}_i, \mu) = b^{-2y_H} C_H(t/b; g_i', \hat{m}_i', \mu), \quad (1)$$

where y_H is the scaling dimension of H [38, 39]. As b increases the fermion mass increases and the fermions decouple from the IR dynamics around $\hat{m}_i' = \mathcal{O}(1)$, i.e.

when the mass is above the cutoff. In RG language this is the scale identified as the IR scale, Λ_{IR} .

In our model we assume two different fermion masses, $\hat{m}_h = am_h$ and $\hat{m}_\ell = am_\ell$, $\hat{m}_h \geq \hat{m}_\ell$. Since both masses scale with the same exponent y_m , the dependence on $\hat{m}_i' = (\hat{m}_h', \hat{m}_\ell')$ in Eq. (1) can be replaced with $(\hat{m}_h', \hat{m}_\ell'/\hat{m}_h) = (\hat{m}_h', m_\ell/m_h)$

$$C_H(t; g_i, \hat{m}_i, \mu) = b^{-2y_H} C_H(t/b; g_i', \hat{m}_h', m_\ell/m_h, \mu). \quad (2)$$

The heavy fermions decouple when $\hat{m}_h' = b^{y_m} \hat{m}_h = \mathcal{O}(1)$, and below that scale any dependence on \hat{m}_h is through the ratio m_ℓ/m_h . We can identify this scale as the UV scale Λ_{UV} which is much lower than the cutoff scale set by the lattice spacing, $\Lambda_{\text{cut}} \approx 1/a$. The light flavors still set the IR scale at $b = \hat{m}_\ell^{-1/y_m}$ and Eq. (2) reduces to

$$C_H(t; g_i, \hat{m}_i, \mu) = \hat{m}_\ell^{2y_H/y_m} C_H(t\hat{m}_\ell^{1/y_m}; g_i', m_\ell/m_h, \mu). \quad (3)$$

Any correlation function is expected to show exponential behavior at large distances,

$$C_H(t; g_i, \hat{m}_i, \mu) \propto e^{-M_H t}, \quad t \rightarrow \infty. \quad (4)$$

Comparing the t dependence of Eqs. (3) and (4) leads to the scaling relation

$$aM_H = (\hat{m}_\ell)^{1/y_m} F_H(m_\ell/m_h), \quad (5)$$

where F_H is some function of m_ℓ/m_h only, assuming b is large enough that the gauge couplings take their IRFP value, $g_i' = g_i^*$. Ratios of masses

$$\frac{M_{H1}}{M_{H2}} = \frac{F_{H1}(m_\ell/m_h)}{F_{H2}(m_\ell/m_h)} \quad (6)$$

depend only on m_ℓ/m_h , though the scaling function F_{H1}/F_{H2} is different for different observables. Between the IR and UV scales the system describes N_ℓ chirally broken fermions, yet the influence of the N_h heavy flavors is still evident though the universal dependence on m_ℓ/m_h and the scaling exponent y_m in Eq. (5). This scaling behavior is unlike in QCD and the consequence of the conformal IRFP that governs the system between the cutoff and UV scales.

In our scaling tests we consider ratios of light-light and heavy-heavy hadrons and find that predictions for different (m_ℓ, m_h) fall on universal curves as function of m_ℓ/m_h . We expect the same to hold for the heavy-light spectrum but did not verify it by numerical simulations. Small deviations from universality can arise from corrections to scaling due to the slowly running gauge coupling, i.e. deviations from $g_i' = g_i^*$. We have investigated these corrections within the $N_f = 12$ system [40].

Increasing m_h will drive the system out of the basin of attraction of the IRFP. Scaling violations start to grow, higher order corrections contribute to γ_m as well as Eqs. (5) and (6). The gauge coupling becomes a relevant parameter, thus the functions F_H depend on g^2 , and the system becomes QCD-like.

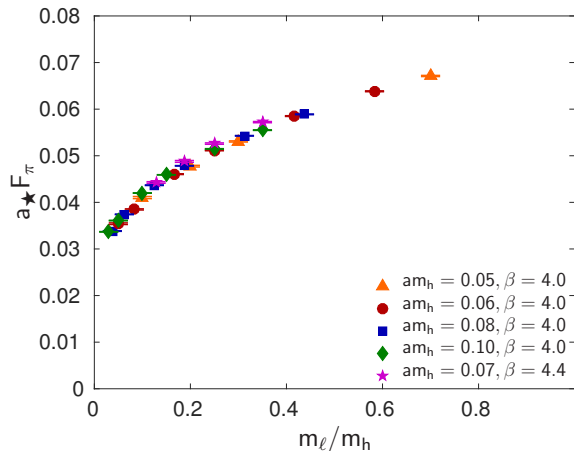


FIG. 1. Dependence of the light-light decay constant F_π in units of a_\star on the hyperscaling variable m_ℓ/m_h (error bars are statistical only). Different colors and symbols correspond to different \hat{m}_h and β values.

III. NUMERICAL RESULTS

Our lattice model is based on $SU(3)$ gauge fields and four light and eight heavy flavors of fundamental fermions. We use staggered fermions with nHYP smearing and the Wilson plaquette gauge action with fundamental and adjoint terms [46–48]. In the IR, the system corresponds, e.g., to the composite Higgs model of Ref. [32], while in the UV it describes the conformal system of 12 degenerate flavors.¹

We investigate the model at two values of the gauge coupling β : At $\beta = 4.0$ we ran simulations using four different values of the heavy mass $\hat{m}_h = 0.05, 0.06, 0.08$ and 0.100 , while at $\beta = 4.4$ we simulate with heavy mass $\hat{m}_h = 0.07$. For each heavy mass \hat{m}_h , we simulate 4 to 6 \hat{m}_ℓ values. Numerical simulations are carried out using FUEL/qhmc [60, 61]. In a conformal system the gauge coupling is irrelevant, the scale or lattice spacing depends on the fermion masses \hat{m}_ℓ and \hat{m}_h . We use the gradient flow scale [62, 63] to convert our data to the same lattice unit denoted by a_\star which we choose to match to the lattice spacing of the ensemble with $(\beta, \hat{m}_\ell, \hat{m}_h) = (4.0, 0.003, 0.080)$. For a first test on hyperscaling, we show $a_\star F_\pi$ as function of the dimensionless ratio m_ℓ/m_h in Fig. 1. As predicted, the 26 independent ensembles — corresponding to different \hat{m}_h and

β values — map out a unique trajectory. The pion decay constant is a particularly important quantity when considering the embedding of the Standard Model in a BSM system because F_π is directly related to the vev of the SM: $F_\pi = vev/\sin\chi$, where $\sin\chi$ is the vacuum alignment angle of composite Higgs systems ($\sin\chi = 1$ in the dilaton-like scenario). The behavior of F_π shown in Fig. 1 not only supports hyperscaling, it also demonstrates that the $4\ell + 8h$ model is chirally broken with finite F_π in the chiral limit.

We continue our study of hyperscaling by investigating light-light and heavy-heavy pseudoscalar, vector, and axial resonances. Figure 2 (wide panels) show dimensionless ratios of their masses in units of F_π as function of m_ℓ/m_h . As expected from hyperscaling, all states at both gauge couplings follow unique curves. Considering the limit $m_\ell/m_h \rightarrow 1$ (degenerate 12 flavors), both heavy-heavy and light-light values approach the $N_f = 12$ values [40–43] as depicted in the small panels to the right. Taking the limit $m_\ell/m_h \rightarrow 0$, we show for comparison PDG values [44] for QCD on the small panels to the left including resonances dominated by $(s\bar{s})$ and charmonium states. While the light-light states match the QCD values closely, the heavy-heavy spectrum is qualitatively different:

- Due to the presence of an IRFP, ratios of heavy-heavy resonances exhibit hyperscaling and are independent of both the gauge coupling and m_h ²
- Heavy-heavy resonances exhibit a significant dependence on the light sea quark mass
- The heavy-heavy resonances are only about a factor 2 – 3 heavier than the light-light states
- Although not measured, heavy-light states are expected to show the same hyperscaling and lie between the light-light and heavy-heavy spectrum

Small corrections to the overall behavior arise from scaling violations (corrections to scaling) due to lattice artifacts. Hyperscaling is only expected if the irrelevant gauge couplings take their fixed point values, $g'_i = g_i^\star$, in Eq. (3). For slowly evolving gauge couplings this could require a large scale change since $b \approx \hat{m}_h^{-1/y_m}$, i.e. small m_h values. Corrections to scaling were investigated and found to be significant for 12 degenerate flavors [40]. Further, the 2-point functions leading to the data shown in Fig. 2 are subject to discretization errors of the fermion action. These discretization errors are known to grow for increasing quark masses. In case of the ratios over F_π , these errors largely cancel for the light-light resonances

¹ The $N_f = 12$ flavor model has been investigated by different groups using lattice techniques [40–42, 48–56]. Most results are in agreement, concluding that $N_f = 12$ is conformal but concerns were raised in Refs. [42, 56]. A new step scaling study [57] addresses those concerns and identifies an infrared fixed point. Further, conformality is supported by a recent study of 10 fundamental flavors using domain-wall fermions that also identifies an IRFP [58, 59]. If $N_f = 10$ is conformal, $N_f = 12$ must be conformal, too.

² This is to be contrasted with QCD where heavy hadron masses are approximately proportional to the sum of the constituent quark masses, as observed by experiment and also in lattice simulations.

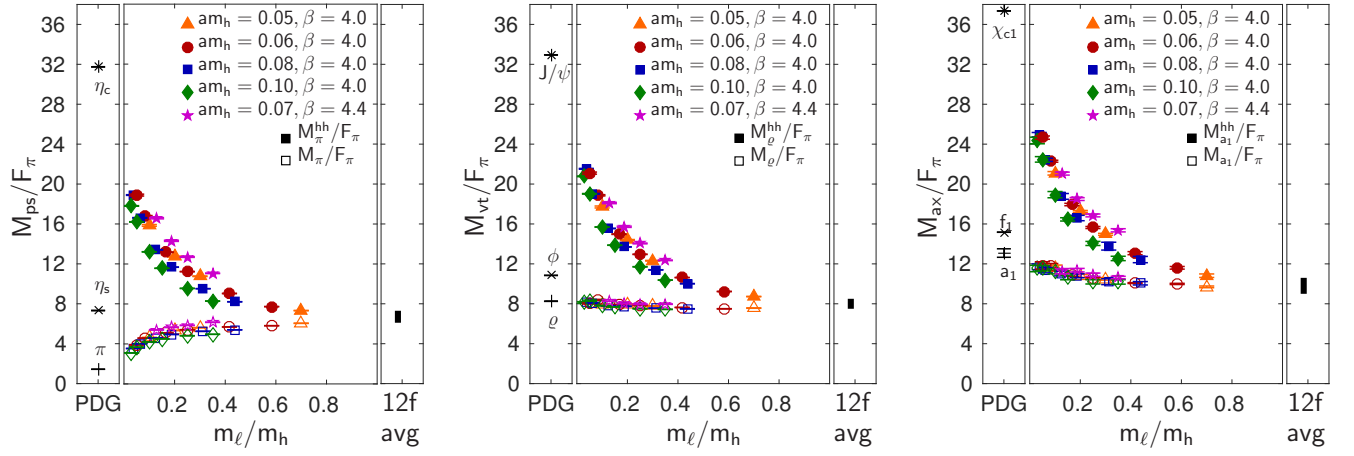


FIG. 2. The three set of panels show dimensionless ratios for pseudoscalar (ps), vector (vt), and axial (ax) meson masses in units of F_π . The wide central panels show our data (with statistical errors only) as function of m_ℓ/m_h . Different colors and symbols indicate the different m_h and β values, while filled (open) symbols denote states of the heavy-heavy (light-light) spectrum. The small panels to the right show averaged values for degenerate 12 flavors [40–43] and the panels on the left the corresponding PDG values [44] for QCD divided by $F_\pi = 94$ MeV. Values for the corresponding bottomonium states (η_b , Υ , and χ_{b1}) are too heavy to be shown on a reasonable scale. While the pseudoscalar and vector states are in general well understood in QCD, pure ($s\bar{s}$) states do not occur in nature. For the η_s mass, we use the lattice determination, $M_{\eta_s} = 688.5(2.2)$ MeV [45], and quote for the vector and axial the PDG entries for the $\phi(1020)$ and $f_1(1420)$, respectively. Regardless of ambiguities in the QCD values, these plots highlight the different character of our heavy-heavy spectrum. Due to the presence of an IRFP, the system shows hyperscaling and we observe independence of the m_h , an unusual behavior in QCD standards.

because discretization errors in numerator and denominator are similar, whereas in case of the heavy-heavy resonances this is not the case, leading to the somewhat larger “scatter” in the heavy-heavy data points.

To understand this better, we show in Fig. 3 the ratios of heavy-heavy pseudoscalar and axial masses over the light-light rho mass (left plot) and the heavy-heavy rho mass (right plot).³ Both plots show hyperscaling in m_h . While the ratios over the light-light M_ρ again introduces a strong dependence on m_ℓ , the m_ℓ dependence is almost entirely canceled when plotting the ratios over M_ρ^{hh} . In that case, also the scatter of the data points is reduced because now there is a better cancellation of discretization errors in the heavy-heavy quantities. However, some scaling violations, especially for the pseudoscalar state remain.

The curve collapse of the different m_h spectra demonstrated in Figs. 2 and 3 is the consequence of hyperscaling at the conformal IRFP. We expect strong violation of this scaling as m_h increases beyond the basin of attraction of the conformal IRFP. Eventually the spectrum could become similar to QCD where light and heavy flavor masses can be tuned independently around the perturbative Gaussian fixed point.

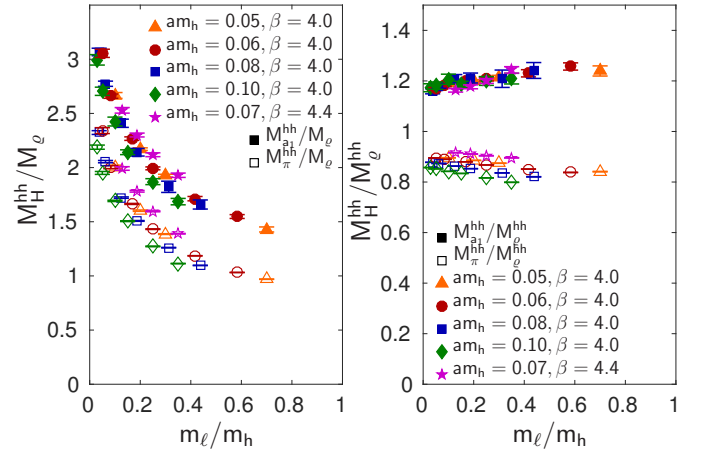


FIG. 3. Mass of the heavy-heavy pseudoscalar (pion) and axial (a_1) shown as ratios over the light-light vector mass M_ρ (left) and the heavy-heavy vector mass M_ρ^{hh} (right) as function of m_ℓ/m_h (statistical errors only). Hyperscaling is present in both plots, but when dividing by M_ρ^{hh} , the dependence on m_ℓ cancels almost entirely and discretization errors are reduced.

IV. OUTLOOK AND CONCLUSION

In this work we investigate systems where the fermions are split into N_h heavy and N_ℓ light flavors. These models are examples for systems with large scale separation if the massless system with $N_f = N_\ell + N_h$ flavors is conformal, while only N_ℓ massless flavors are chirally broken. In the UV where all flavor masses are much lighter than

³ Both $\rho^{\ell\ell}$ and ρ^{hh} are stable since in our simulations they are energetically not allowed to decay to two pions.

the energy scale, the flavors can be considered degenerate and the dynamics is controlled by the conformal fixed point. Once the energy scale drops below the heavy flavor mass, the heavy flavors decouple and in the IR the system is chirally broken with only N_ℓ light flavors. The scale separation is fully controlled by the mass of the heavy flavors.

Hyperscaling relations at the conformal fixed point control the scaling behavior of the light-light, heavy-light, and heavy-heavy resonance spectrum. General Wilsonian renormalization group considerations imply that dimensionless ratios depend only on the ratio of the flavor masses m_ℓ/m_h and not their individual values. This behavior is the consequence of the conformal fixed point and is very different from the well understood QCD case. This property of mass-split systems is general and applies to similar models.

We have verified the hyperscaling expectations in numerical simulations with our model of four light and eight heavy flavors. We found that the heavy-heavy spectrum is only a couple of times heavier than the light-light one and independent of the heavy fermion mass. This property of the heavy-heavy spectrum is fundamentally different from what is observed in QCD where quarkonia masses are proportional to the constituent quark mass. Furthermore, we observe that light-light but also heavy-heavy resonances are subject to large sea-quark mass effects; in QCD those effects are, in particular for heavy-heavy states, largely suppressed.

If this system describes BSM phenomenology with the light-light resonances in the few TeV range, the heavy-

light and heavy-heavy states would be within the LHC range as well. Discriminating the various BSM models is however challenging because the light-light spectrum shows little changes overall when varying the number of flavors or fermion representations [7, 19–22]. It is therefore interesting to investigate how the heavy-heavy or heavy-light spectrum changes with the number of flavors that changes the anomalous dimension of the conformal fixed point in the UV.

ACKNOWLEDGMENTS

The authors thank their colleagues in the LSD Collaboration for fruitful and inspiring discussions. Computations for this work were carried out in part on facilities of the USQCD Collaboration, which are funded by the Office of Science of the U.S. Department of Energy, on computers at the MGHPCC, in part funded by the National Science Foundation (award OCI-1229059), and on computers allocated under the NSF Xsede program to the project TG-PHY120002. We thank Boston University, Fermilab, the NSF and the U.S. DOE for providing the facilities essential for the completion of this work. A.H. acknowledges support by DOE grant DE-SC0010005 and C.R. by DOE grant DE-SC0015845. This project has received funding from the European Union’s Horizon 2020 research and innovation programme under the Marie Skłodowska-Curie grant agreement No 659322.

-
- [1] D. Charlton, “Highlights from the LHC (I),” (2016), plenary talk at ICHEP 2016, Chicago.
 - [2] T. Camporesi, “LHC results Highlights,” (2016), plenary talk at ICHEP 2016, Chicago.
 - [3] R. Contino, *Proceedings TASI* **09**, 235 (2011), [arXiv:1005.4269 \[hep-ph\]](#).
 - [4] M. A. Luty and T. Okui, *JHEP* **09**, 070 (2006), [arXiv:hep-ph/0409274 \[hep-ph\]](#).
 - [5] D. D. Dietrich and F. Sannino, *Phys. Rev.* **D75**, 085018 (2007), [arXiv:hep-ph/0611341 \[hep-ph\]](#).
 - [6] M. A. Luty, *JHEP* **04**, 050 (2009), [arXiv:0806.1235 \[hep-ph\]](#).
 - [7] R. C. Brower, A. Hasenfratz, C. Rebbi, E. Weinberg, and O. Witzel, *Phys. Rev.* **D93**, 075028 (2016), [arXiv:1512.02576 \[hep-ph\]](#).
 - [8] C. Csaki, C. Grojean, and J. Terning, *Rev. Mod. Phys.* **88**, 045001 (2016), [arXiv:1512.00468 \[hep-ph\]](#).
 - [9] N. Arkani-Hamed, R. T. D’Agnolo, M. Low, and D. Pinner, *JHEP* **11**, 082 (2016), [arXiv:1608.01675 \[hep-ph\]](#).
 - [10] A. Hasenfratz, C. Rebbi, and O. Witzel, *PoS LATTICE2016*, 226 (2016), [arXiv:1611.07427 \[hep-lat\]](#).
 - [11] A. Hasenfratz, C. Rebbi, and O. Witzel, in preparation (2017).
 - [12] S. Weinberg, *Phys. Rev.* **D19**, 1277 (1979).
 - [13] L. Susskind, *Phys. Rev.* **D20**, 2619 (1979).
 - [14] E. Eichten and K. D. Lane, *Phys. Lett.* **B90**, 125 (1980).
 - [15] B. Holdom, *Phys. Lett.* **B150**, 301 (1985).
 - [16] K. Yamawaki, M. Bando, and K.-i. Matumoto, *Phys. Rev. Lett.* **56**, 1335 (1986).
 - [17] M. Bando, T. Kugo, and K. Yamawaki, *Phys. Rept.* **164**, 217 (1988).
 - [18] T. Appelquist, J. Terning, and L. C. R. Wijewardhana, *Phys. Rev. D* **44**, 871 (1991).
 - [19] Y. Aoki, T. Aoyama, M. Kurachi, T. Maskawa, K. Miura, K.-i. Nagai, H. Ohki, E. Rinaldi, A. Shibata, K. Yamawaki, and T. Yamazaki (LatKMI), *Phys. Rev.* **D89**, 111502 (2014), [arXiv:1403.5000 \[hep-lat\]](#).
 - [20] Y. Aoki, T. Aoyama, M. Kurachi, T. Maskawa, K.-i. Nagai, H. Ohki, A. Shibata, K. Yamawaki, and T. Yamazaki (LatKMI), *Phys. Rev.* **D87**, 094511 (2013), [arXiv:1302.6859 \[hep-lat\]](#).
 - [21] T. Appelquist, R. Brower, G. Fleming, A. Hasenfratz, X.-Y. Jin, J. Kiskis, E. Neil, J. Osborn, C. Rebbi, E. Rinaldi, D. Schaich, P. Vranas, E. Weinberg, and O. Witzel, *Phys. Rev.* **D93**, 114514 (2016), [arXiv:1601.04027 \[hep-lat\]](#).
 - [22] Z. Fodor, K. Holland, J. Kuti, D. Negradi, and C. H. Wong, *PoS LATTICE2013*, 062 (2014), [arXiv:1401.2176 \[hep-lat\]](#).
 - [23] Z. Fodor, K. Holland, J. Kuti, S. Mondal, D. Negradi, and C. H. Wong, *Phys. Rev.* **D94**, 014503 (2016), [arXiv:1601.03302 \[hep-lat\]](#).

- [24] T. DeGrand, *Rev. Mod. Phys.* **88**, 015001 (2016), [arXiv:1510.05018 \[hep-ph\]](#).
- [25] D. Negradi and A. Patella, *Int. J. Mod. Phys. A* **31**, 1643003 (2016), [arXiv:1607.07638 \[hep-lat\]](#).
- [26] D. B. Kaplan and H. Georgi, *Phys. Lett.* **B136**, 183 (1984).
- [27] D. B. Kaplan, H. Georgi, and S. Dimopoulos, *Phys. Lett.* **B136**, 187 (1984).
- [28] M. J. Dugan, H. Georgi, and D. B. Kaplan, *Nucl. Phys.* **B254**, 299 (1985).
- [29] K. Agashe, R. Contino, and A. Pomarol, *Nucl. Phys.* **B719**, 165 (2005), [arXiv:hep-ph/0412089 \[hep-ph\]](#).
- [30] G. Ferretti and D. Karateev, *JHEP* **03**, 077 (2014), [arXiv:1312.5330 \[hep-ph\]](#).
- [31] G. Ferretti, *JHEP* **06**, 142 (2014), [arXiv:1404.7137 \[hep-ph\]](#).
- [32] T. Ma and G. Cacciapaglia, *JHEP* **03**, 211 (2016), [arXiv:1508.07014 \[hep-ph\]](#).
- [33] L. Vecchi, (2015), [arXiv:1506.00623 \[hep-ph\]](#).
- [34] D. Buarque Franzosi, G. Cacciapaglia, H. Cai, A. Deandrea, and M. Frandsen, (2016), [arXiv:1605.01363 \[hep-ph\]](#).
- [35] A. Hietanen, R. Lewis, C. Pica, and F. Sannino, *JHEP* **07**, 116 (2014), [arXiv:1404.2794 \[hep-lat\]](#).
- [36] R. Arthur, V. Drach, M. Hansen, A. Hietanen, C. Pica, and F. Sannino, *Phys. Rev.* **D94**, 094507 (2016), [arXiv:1602.06559 \[hep-lat\]](#).
- [37] T. A. DeGrand, D. Hackett, W. I. Jay, E. T. Neil, Y. Shamir, and B. Svetitsky, *PoS LATTICE2016*, 219 (2016), [arXiv:1610.06465 \[hep-lat\]](#).
- [38] T. DeGrand and A. Hasenfratz, *Phys. Rev.* **D80**, 034506 (2009), [arXiv:0906.1976 \[hep-lat\]](#).
- [39] L. Del Debbio and R. Zwicky, *Phys. Rev.* **D82**, 014502 (2010), [arXiv:1005.2371 \[hep-ph\]](#).
- [40] A. Cheng, A. Hasenfratz, Y. Liu, G. Petropoulos, and D. Schaich, *Phys. Rev.* **D90**, 014509 (2014), [arXiv:1401.0195 \[hep-lat\]](#).
- [41] Y. Aoki, T. Aoyama, M. Kurachi, T. Maskawa, K.-i. Nagai, H. Ohki, A. Shibata, K. Yamawaki, and T. Yamazaki (LatKMI), *Phys. Rev.* **D86**, 054506 (2012), [arXiv:1207.3060 \[hep-lat\]](#).
- [42] Z. Fodor, K. Holland, J. Kuti, D. Negradi, C. Schroeder, K. Holland, J. Kuti, D. Negradi, and C. Schroeder, *Phys. Lett.* **B703**, 348 (2011), [arXiv:1104.3124 \[hep-lat\]](#).
- [43] Y. Aoki, T. Aoyama, M. Kurachi, T. Maskawa, K.-i. Nagai, H. Ohki, E. Rinaldi, A. Shibata, K. Yamawaki, and T. Yamazaki (LatKMI), *Phys. Rev. Lett.* **111**, 162001 (2013), [arXiv:1305.6006 \[hep-lat\]](#).
- [44] K. A. Olive et al. (Particle Data Group), *Chin. Phys.* **C38**, 090001 (2014).
- [45] R. J. Dowdall, C. T. H. Davies, G. P. Lepage, and C. McNeile, *Phys. Rev.* **D88**, 074504 (2013), [arXiv:1303.1670 \[hep-lat\]](#).
- [46] A. Hasenfratz and F. Knechtli, *Phys. Rev.* **D64**, 034504 (2001), [arXiv:hep-lat/0103029](#).
- [47] A. Hasenfratz, R. Hoffmann, and S. Schaefer, *JHEP* **0705**, 029 (2007), [arXiv:hep-lat/0702028 \[hep-lat\]](#).
- [48] A. Hasenfratz, *Phys. Rev. Lett.* **108**, 061601 (2012), [arXiv:1106.5293 \[hep-lat\]](#).
- [49] T. DeGrand, *Phys. Rev.* **D84**, 116901 (2011), [arXiv:1109.1237 \[hep-lat\]](#).
- [50] A. Cheng, A. Hasenfratz, G. Petropoulos, and D. Schaich, *JHEP* **1307**, 061 (2013), [arXiv:1301.1355 \[hep-lat\]](#).
- [51] K. I. Ishikawa, Y. Iwasaki, Y. Nakayama, and T. Yoshie, *Phys. Rev.* **D89**, 114503 (2014), [arXiv:1310.5049 \[hep-lat\]](#).
- [52] A. Cheng, A. Hasenfratz, Y. Liu, G. Petropoulos, and D. Schaich, *JHEP* **1405**, 137 (2014), [arXiv:1404.0984 \[hep-lat\]](#).
- [53] M. P. Lombardo, K. Miura, T. J. N. da Silva, and E. Pallante, *JHEP* **12**, 183 (2014), [arXiv:1410.0298 \[hep-lat\]](#).
- [54] M. P. Lombardo, K. Miura, T. J. Nunes da Silva, and E. Pallante, *PoS CPOD2014*, 059 (2015), [arXiv:1506.05946 \[hep-lat\]](#).
- [55] C. J. D. Lin, K. Ogawa, and A. Ramos, *JHEP* **12**, 103 (2015), [arXiv:1510.05755 \[hep-lat\]](#).
- [56] Z. Fodor, K. Holland, J. Kuti, S. Mondal, D. Negradi, and C. H. Wong, *Phys. Rev.* **D94**, 091501 (2016), [arXiv:1607.06121 \[hep-lat\]](#).
- [57] A. Hasenfratz and D. Schaich, (2016), [arXiv:1610.10004 \[hep-lat\]](#).
- [58] T.-W. Chiu, (2016), [arXiv:1603.08854 \[hep-lat\]](#).
- [59] T.-W. Chiu, *PoS LATTICE2016*, 228 (2017).
- [60] J. Osborn, *PoS LATTICE2014*, 028 (2014).
- [61] J. Osborn et al., “Framework for unified evolution of lattices (FUEL),” .
- [62] M. Lüscher, *JHEP* **1008**, 071 (2010), [arXiv:1006.4518 \[hep-lat\]](#).
- [63] A. Hasenfratz, *PoS LATTICE2014*, 257 (2015), [arXiv:1501.07848 \[hep-lat\]](#).